NADPH oxidase mediates oxidative stress in the 1-methyl-4-phenyl-1,2,3,6-tetrahydropyridine model of Parkinson's disease

Du-Chu Wu*, Peter Teismann*, Kim Tieu*, Miquel Vila*, Vernice Jackson-Lewis*, Harry Ischiropoulos†, and Serge Przedborski*‡§¶

Departments of *Neurology and ‡Pathology and §Center for Neurobiology and Behavior, Columbia University, New York, NY 10032; and †Stokes Research Institute, Department of Pediatrics, Children's Hospital of Philadelphia, and Department of Biochemistry and Biophysics, University of Pennsylvania School of Medicine, Philadelphia, PA 19104

Edited by Tomas Hökfelt, Karolinska Institute, Stockholm, Sweden, and approved March 13, 2003 (received for review November 27, 2002)

Parkinson's disease (PD) is a neurodegenerative disorder of uncertain pathogenesis characterized by a loss of substantia nigra pars compacta (SNpc) dopaminergic (DA) neurons, and can be modeled by the neurotoxin 1-methyl-4-phenyl-1,2,3,6-tetrahydropyridine (MPTP). Both inflammatory processes and oxidative stress may contribute to MPTP- and PD-related neurodegeneration. However, whether inflammation may cause oxidative damage in MPTP and PD is unknown. Here we show that NADPH-oxidase, the main reactive oxygen species (ROS)-producing enzyme during inflammation, is up-regulated in SNpc of human PD and MPTP mice. These changes coincide with the local production of ROS, microglial activation, and DA neuronal loss seen after MPTP injections. Mutant mice defective in NADPH-oxidase exhibit less SNpc DA neuronal loss and protein oxidation than their WT littermates after MPTP injections. We show that extracellular ROS are a main determinant in inflammation-mediated DA neurotoxicity in the MPTP model of PD. This study supports a critical role for NADPH-oxidase in the pathogenesis of PD and suggests that targeting this enzyme or enhancing extracellular antioxidants may provide novel therapies for PD.

Parkinson's disease (PD) is a common neurodegenerative disease characterized by disabling motor abnormalities, which include tremor, muscle stiffness, paucity of voluntary movements, and postural instability (1). Its main neuropathological feature is the loss of the nigrostriatal dopamine (DA)-containing neurons, whose cell bodies are in the substantia nigra pars compacta (SNpc) and nerve terminals are in the striatum (2). Except for a handful of inherited cases related to known gene defects, PD is a sporadic condition of unknown pathogenesis (1).

Epidemiological studies suggest that inflammation increases the risk of developing PD (3). Consistent with this view, experimental models of PD show that inflammatory factors may trigger or modulate SNpc DA neuronal death (4–6). Among inflammatory mediators capable of promoting neurodegeneration are microglial-derived reactive oxygen species (ROS). These may deserve particular attention, because oxidative stress is a leading pathogenic hypothesis of PD (7).

A significant source of ROS during inflammation is NADPH-oxidase, which is a multimeric enzyme composed of $gp91^{phox}$, $p22^{phox}$, $p47^{phox}$, $p67^{phox}$, and $p40^{phox}$ subunits (8). In resting microglia, NADPH-oxidase is inactive because $p47^{phox}$, $p67^{phox}$, and $p40^{phox}$, which are present in the cytosol as a complex, are separated from $gp91^{phox}$ and $p22^{phox}$, which are transmembrane proteins. Upon microglial activation, $p47^{phox}$ becomes phosphorylated and the entire cytosolic complex translocates to the membrane, where it assembles with $gp91^{phox}$ and $p22^{phox}$, thus forming a NADPH-oxidase entity now capable of reducing oxygen to superoxide radical (O_2^-), which in turn gives rise to the production of other secondary reactive oxidants (8).

Although NADPH-oxidase is critical to the killing of invading microorganisms in infections through its abundant and sustained production of O_2^- (8), its role in noninfectious chronic neurodegenerative processes, such as PD, is not known. In the present study, we show not only that the NADPH-oxidase main subunit $gp91^{phox}$ is up-regulated in the SNpc of PD and 1-methyl-4-phenyl-1,2,3,6-tetrahydropyridine (MPTP) mice, but also that NADPH-oxidase inactivation attenuates MPTP neurotoxicity by mitigating inflammation-mediated oxidative attack on SNpc neurons. These findings indicate that NADPH-oxidase-induced oxidative stress is instrumental in SNpc DA neurodegeneration caused by MPTP, and suggest that NADPH-oxidase is a valuable therapeutic target for the development of neuroprotective strategies for PD.

Materials and Methods

Animals and Treatment. Eight-week-old male C57BL/6 mice (Charles River Breeding Laboratories), $gp91^{phox}$-deficient mice (B6.129S6-$Cybb^{tm1din}$, The Jackson Laboratory), and their WT littermates were used. Mice received four i.p. injections of MPTP-HCl (16 mg/kg free base; Sigma) dissolved in saline at 2-h intervals, and were killed 0–14 days after the last injection. Control mice received saline only. MPTP handling and safety measures were in accordance with our published guidelines (9). Minocycline (2×45 mg/kg per day; Sigma) was given to MPTP mice as described (5). Bovine erythrocyte superoxide dismutase 1 (SOD1; 20 units/h; Sigma) was infused into the left striatum with an osmotic minipump (Alzet, Palo Alto, CA) starting 1 day before and stopping 6 days after the MPTP injections. This protocol was in accordance with the National Institutes of Health guidelines for use of live animals and was approved by the Institutional Animal Care and Use Committee of Columbia University (New York). Striatal 1-methyl-4-phenylpyridinium levels were determined by HPLC as described (5).

RNA Extraction and RT-PCR. Total RNA was extracted as described (5). The primer mouse sequences were as follows: $gp91^{phox}$, 5′-CAGGAGTTCCAAGATGCCTG-3′ (forward) and 5′-GATTGGCCTGAGATTCATCC-3′ (reverse); $p67^{phox}$, 5′-CAGCCAGCTTCGGAACATG-3′ (forward) and 5′-GACAGTACCAGGATTACATC-3′ (reverse); macrophage antigen complex 1 (Mac-1), 5′-TTCTCATGGTCACCTCCTGC-3′ (forward) and 5′-GGTCTGACCATCTGAACCTG-3′ (reverse); GAPDH, 5′-GTTTCTTACTCCTTGGAGGCCAT-3′ (forward) and 5′-TGATGACATCAAGAAGTGGTGAA-3′ (reverse). PCR was carried out for 29 cycles for $gp91^{phox}$, 27 cycles for $p67^{phox}$ and Mac-1, and 20 cycles for GAPDH. Each cycle

This paper was submitted directly (Track II) to the PNAS office.

Abbreviations: Mac-1, macrophage antigen complex 1; MPTP, 1-methyl-4-phenyl-1,2,3,6-tetrahydropyridine; PD, Parkinson's disease; ROS, reactive oxygen species; SNpc, substantia nigra pars compacta; TH, tyrosine hydroxylase; DA, dopamine/dopaminergic; SOD1, superoxide dismutase 1.

¶To whom correspondence should be addressed. E-mail: sp30@columbia.edu.

consisted of 30 s of denaturation at 94°C, 40 s of annealing at 55°C, and 60 s of extension at 72°C, followed by a final 7-min extension at 72°C. Products were quantified by a phosphor imager (Bio-Rad).

Digoxigenin-Labeled cRNA Probe and *in Situ* Hybridization. Antisense and sense RNA probes were prepared by *in vitro* transcription from a mouse gp91^{phox} cDNA fragment (nucleotides 1020–1493; GenBank accession no. U43384) by using SP6/T7 RNA polymerase in the presence of digoxigenin-linked UTP (Roche Molecular Biochemicals) according to the supplier's instructions. Frozen midbrain sections (14 μm thick) were incubated with the antisense or sense (for control) digoxigenin-labeled probes. Hybridization signal was detected by 5-bromo-4-chloro-indolyl-phosphatase and nitroblue tetrazolium.

Immunohistochemistry and Quantitative Morphology. Mouse brains were fixed and processed for immunostaining as described (5). Primary Abs were as follows: for mouse sections, monoclonal anti-mouse gp91^{phox} (1:1,000; Transduction Laboratories, Lexington, KY), rat anti-MAC-1 (1:200; Serotec), monoclonal anti-tyrosine hydroxylase (TH; 1:1,000; Chemicon), and polyclonal anti-TH (1:1,000; Calbiochem, San Diego); for human sections, monoclonal anti-human gp91^{phox} (gift from Genentech) and monoclonal anti-human CD68 (DAKO). Immunolabeling was visualized by using 3,3′-diaminobenzidine (brown), VECTOR SG (blue/gray), 3-amino-9-ethylcarbazole (red), or fluorescein and Texas red (all from Vector Laboratories).

Total numbers of TH-positive SNpc neurons were counted by stereology by using the optical fractionator method described previously (6). Striatal density of TH immunoreactivity was determined as described (5).

Western Blots. Total, cytosolic, and plasma membrane proteins were prepared as described (5). Primary Abs were as follows: for mouse proteins, monoclonal anti-mouse p67^{phox} (1:1,000; Transduction Laboratories), polyclonal anti-gp91^{phox} (1:5,000, gift from M. C. Dinauer, Indiana University, Indianapolis), and polyclonal anti-calnexin (1:5,000; Stressgen Biotechnologies, Victoria, Canada); for human proteins, monoclonal anti-human gp91^{phox} (1:500, Genentech). A monoclonal anti-β-actin (1:5,000; Sigma) was used for both mouse and human proteins. Bound primary Ab was detected by using a horseradish peroxidase-conjugated secondary Ab against IgG and a chemiluminescent substrate (SuperSignal Ultra, Pierce). Films were quantified by using the NIH IMAGE analysis system.

***In Situ* Visualization of O_2^- and O_2^--Derived Oxidant Production.** *In situ* visualization of O_2^- and O_2^--derived oxidant production was assessed by hydroethidine histochemistry (10). At selected time points after MPTP administration, mice were injected i.p. with 200 μl of PBS containing 1 μg/μl hydroethidine (Molecular Probes) and 1% DMSO. Brains were harvested 15 min later and frozen on dry ice. Midbrain sections (14 μm thick) mounted onto gelatin-coated glass slides were examined for hydroethidine oxidation product, ethidium accumulation, by fluorescence microscopy (excitation, 510 nm; emission, 580 nm). The same tissue sections were used for Mac-1 immunohistochemistry.

Protein carbonyls were detected after derivatization of brain homogenates with 2,4-dinitrophenylhydrazine by using a modification of the method described by Levine *et al.* (11). The concentration of protein carbonyls was calculated from the difference in absorbance at 360 nm between the underivatized and 2,4-dinitrophenylhydrazine-derivatized samples normalized to the protein concentration. The extinction coefficient of 21 $mM^{-1}\cdot cm^{-1}$ was applied to calculate the concentration of protein carbonyls.

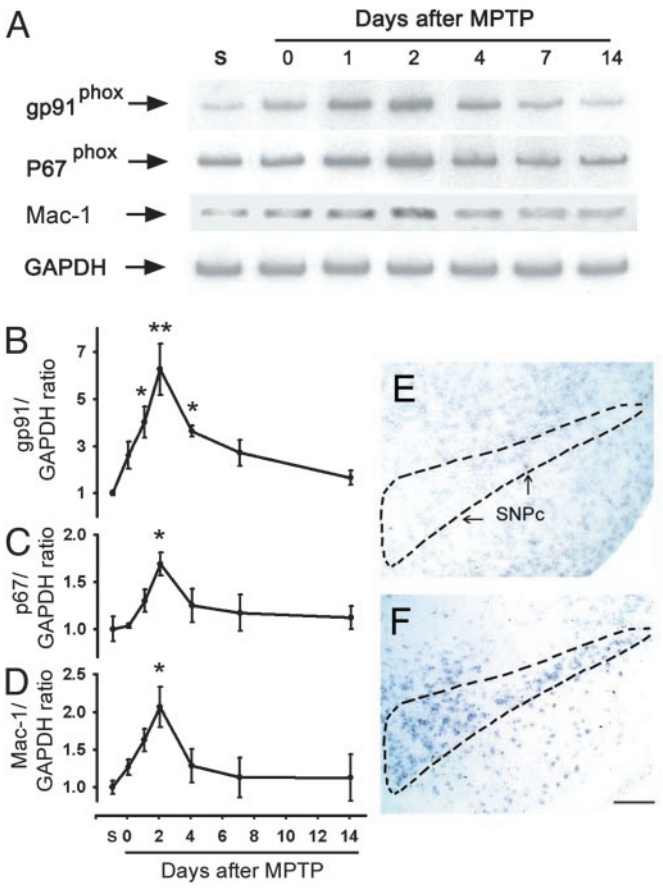

Fig. 1. (*A–D*) RT-PCR shows ventral midbrain gp91^{phox}, p67^{phox}, and Mac-1 mRNA levels in saline-injected (S) and MPTP-injected mice from 0 to 14 days after injections. SNpc gp91^{phox} mRNA labeling is negligible in saline-injected mice (*E*), whereas it is copious in MPTP-injected mice at 2 days (*F*). *, $P < 0.05$; **, $P < 0.001$, more than saline-treated mice ($n = 4–6$ per time point). (Scale, 2.5 mm.)

Human Samples. Age at death and interval from death to tissue processing (mean ± SEM) were as follows: for the control group ($n = 3$), 72.2 ± 8.8 y and 13.0 ± 3.5 h, respectively; for the PD group ($n = 6$), 77.2 ± 2.3 y and 10.1 ± 2.4 h, respectively. For the PD patients, the mean duration of disease was 16.8 ± 2.3 y.

Statistical Analysis. Values represent means ± SEM. Differences among means were analyzed by using one- or two-way ANOVA with time, treatment, or genotype as the independent factors. When ANOVA showed significant differences, pairwise comparisons between means were analyzed by Newman–Keuls post hoc testing. The null hypothesis was consistently rejected at the 0.05 level.

Results

NADPH-Oxidase Is Induced in Mouse Ventral Midbrain During MPTP Neurotoxicity. To define the temporal relationship between NADPH-oxidase expression and MPTP neurotoxicity, contents of ventral midbrain (brain region containing SNpc) membrane-bound subunit gp91^{phox} and cytosolic subunit p67^{phox} mRNA were assessed throughout the time course of MPTP-induced SNpc DA neurodegeneration (12). In saline-injected mice, ventral midbrain gp91^{phox}, p67^{phox}, and Mac-1 (microglial marker) mRNAs were low (Fig. 1 *A–D*). In contrast, in MPTP-injected mice, ventral midbrain gp91^{phox}, p67^{phox}, and Mac-1 mRNAs

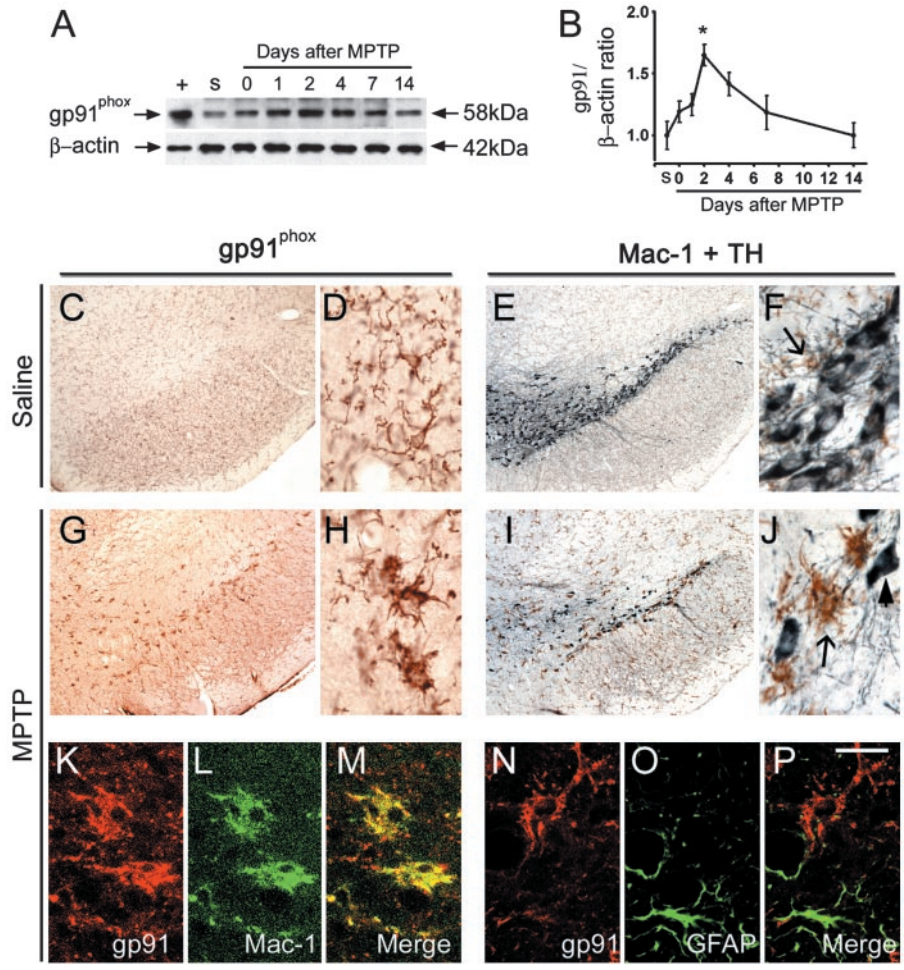

Fig. 2. Western blot shows the time-dependent induction of gp91^{phox} in mouse ventral midbrain after MPTP injections. +, Mouse macrophage lysate; s, saline. In saline-injected mice, gp91^{phox} immunoreactivity (*C* and *D*, brown) is mild and localized in resting microglia, which are not abundant in the SNpc, as shown (*E* and *F*) by Mac-1 labeling (brown, arrow) and are intermingled with TH-positive neurons (gray-blue). Two days after MPTP injections, numerous gp91^{phox}-positive cells are seen in the SNpc (*G* and *H*). These cells resemble activated microglial cells (*H* vs. *J*, arrow). At this point there are many fewer TH-positive neurons (*I* and *J*, arrowhead). Confocal microscopy shows that all gp91^{phox}-positive cells are Mac-1-positive, thus confirming their microglial origin (*K* and *L*). Conversely, no gp91^{phox}-positive cells are glial fibrillary acidic protein-positive cells, thus excluding their astrocytic origin (*N–P*). *, $P < 0.05$, more than saline-treated mice (n = 6 per time point). [Scale bar, 2.5 mm (*C*, *E*, *G*, and *I*); 0.25 mm (*D*, *F*, *H*, and *J*); and 0.2 mm (*K–P*).]

increased in a time-dependent manner after MPTP injections (Fig. 1 *A–D*).

In saline-injected mice, nonradioactive *in situ* hybridization for gp91^{phox}, which is one of the main functional subunits of NADPH-oxidase, revealed no specific labeling in ventral midbrain (Fig. 1*E*), whereas in MPTP-injected mice there was conspicuous specific labeling over the SNpc at 2 days after MPTP injections (Fig. 1*F*). Thus, these results indicate that NADPH-oxidase is induced after MPTP administration specifically in the area where the demise of DA neurons arises in this model of PD.

NADPH-Oxidase Is Expressed in Activated Microglia After MPTP Injection. Consistent with the mRNA data, ventral midbrain gp91^{phox} protein contents rose in a time-dependent manner after MPTP injections (Fig. 2 *A* and *B*). In cell cultures, NADPH-oxidase has been identified in different cell types, including neurons (13). In saline-injected mice, mild gp91^{phox} immunoreactivity was seen throughout the substantia nigra (Fig. 2*C*) without greater gp91^{phox} immunolabeling in the SNpc, which hosts the TH-positive neurons (Fig. 2 *E* and *F*). Immunoreactivity of gp91^{phox} was in small cells with thin ramifications (Fig. 2*D*) reminiscent of resting microglia (Fig. 2*F*). In MPTP-injected mice, robust gp91^{phox} immunoreactivity was seen specifically in the SNpc (Fig. 2*G*) in larger cells with thick, shorter ramifications (Fig. 2*H*) reminiscent of activated microglia (Fig. 2*J*). Similar immunohistochemical gp91^{phox} alterations were seen in the striatum, which contains the nerve terminals of the projecting SNpc DA neurons, between the saline- and MPTP-injected mice (data not shown). By confocal microscopy, gp91^{phox} immunoreactivity appeared to colocalize with Mac-1 (Fig. 2 *K–M*). Conversely, gp91^{phox} immunoreactivity did not colocalize either with the astrocytic marker glial fibrillary acidic protein (Fig. 2 *N–P*) or with TH (data not shown). Thus, these results demonstrate that, after MPTP administration, SNpc microglia become activated at the site of NADPH-oxidase induction.

Expression of gp91^{phox} Is Increased in PD Midbrain. Consistent with the finding in the MPTP mice, postmortem SNpc samples from sporadic PD patients had higher gp91^{phox} protein contents than controls (Fig. 3 *A* and *B*). In these autopsy specimens, cellular gp91^{phox} immunoreactivity was barely identified in controls (Fig. 3*C*) but was strong in PD midbrain sections, where it was identified in microglial cells (Fig. 3*D*). The similarity of the

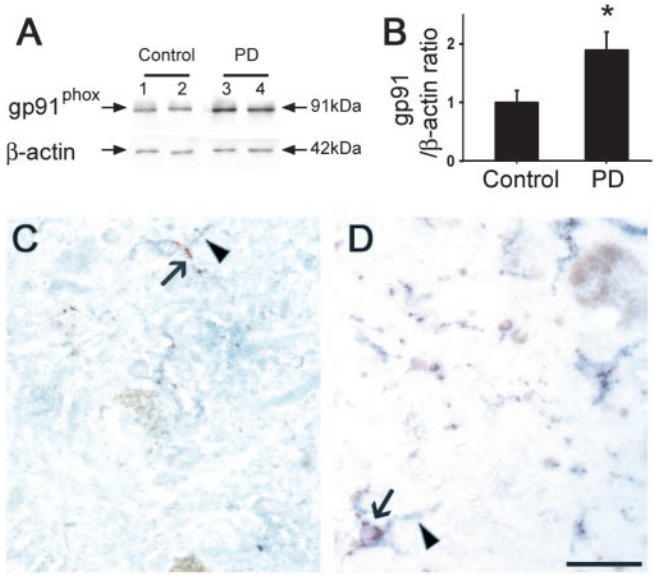

Fig. 3. (*A*) Representative Western blots illustrating the increase in ventral midbrain gp91^{phox} protein content in two PD and two controls. (*B*) Bar graph showing mean Western blot gp91^{phox}/β-actin ratios ± SEM for six PD and three control ventral midbrain samples. (*C* and *D*) Representative gp91^{phox} immunostaining that shows positive cells in PD samples (arrowhead, gray-blue, membrane labeling) colocalizing with the microglial marker CD68 (arrow, red, cytosol labeling), but not with neuromelanin (brown pigment). *, $P < 0.05$, higher than controls. (Scale bar, 0.5 mm.)

gp91^{phox} alterations between the MPTP mice and the PD postmortem specimens validates the use of the MPTP experimental model to study the role of NADPH-oxidase in the PD neurodegenerative process.

The Lack of gp91^{phox} Abates MPTP-Associated ROS Production. In saline-injected mice, ventral midbrain O_2^- and O_2^--derived oxidant production, evidenced by ethidium fluorescence, was minimal (Fig. 4*A*). In contrast, in MPTP-treated mice, ventral midbrain production of O_2^- or O_2^--derived oxidants shown by ethidium fluorescence was increased by 12 h (data not shown), was maximal by 2 days (Fig. 4*C*), and remained elevated at 7 days after MPTP (data not shown). SNpc ethidium fluorescence coincided with the location and the time course of microglial activation seen after MPTP administration (Fig. 4 *C* and *D*).

In mutant mice lacking the gp91^{phox} subunit, no translocation of the cytosolic p67^{phox} subunit to the plasma membrane was seen after MPTP injections (Fig. 4 *I* and *J*), which is mandatory for NADPH-oxidase to become catalytically competent (8). Unlike WT littermates (Fig. 4 *C* and *D*), mutant mice with defective NADPH-oxidase failed to show any increase in SNpc ethidium fluorescence (Fig. 4*E*), despite normal microglial activation after MPTP administration (Fig. 4*F*). WT mice treated with minocycline (i.e., antibiotic that blocks microglial activation) showed no increase in SNpc ethidium fluorescence (Fig. 4*G*) and no microglial activation after MPTP administration (Fig. 4*E*). Thus, these findings demonstrate that during the MPTP neurotoxic process there is an increased production of ROS in the SNpc that originates from activated microglial cells and is mediated by NADPH-oxidase.

NADPH-Oxidase Defect Protects Against MPTP Neurodegeneration. In the ventral midbrain of saline-injected mice, the stereological counts of SNpc TH-positive neurons did not differ between gp91^{phox}-deficient mice and their WT littermates (Fig. 5*A*). In MPTP-injected mice, the numbers of SNpc TH-positive neurons

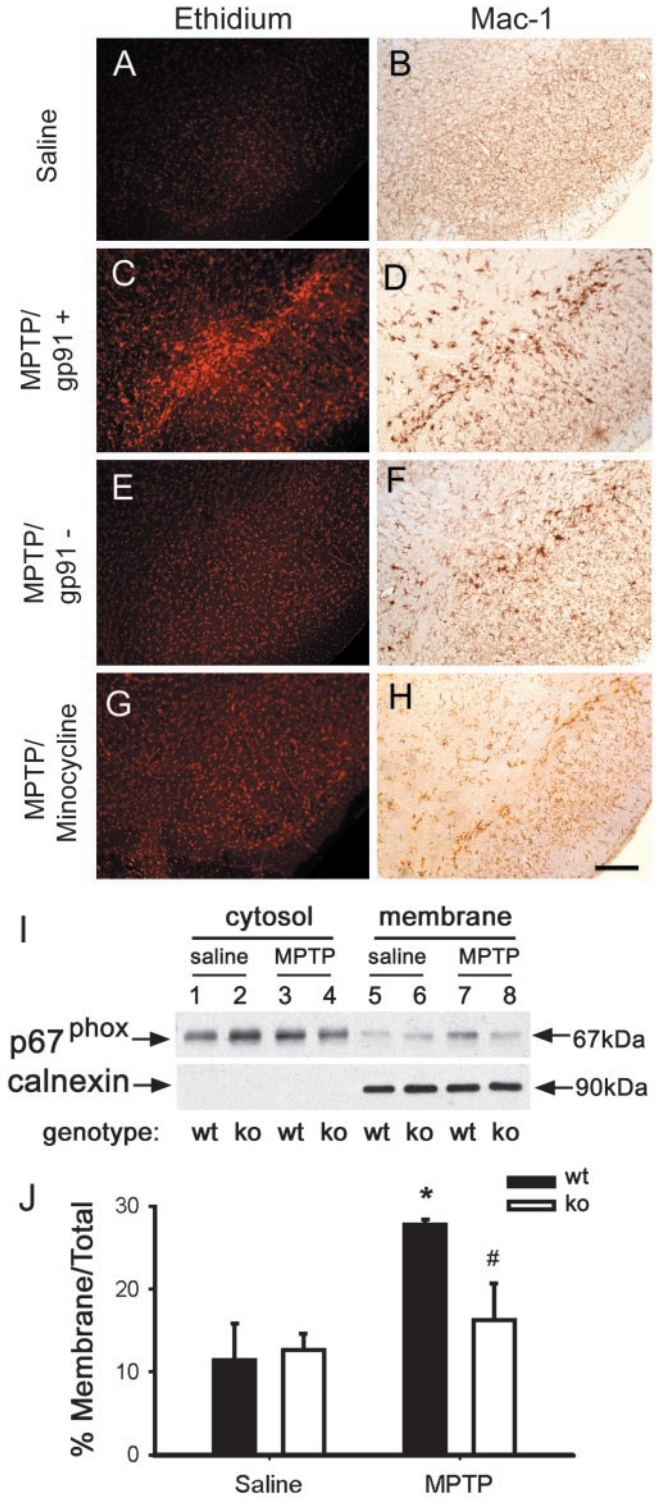

Fig. 4. Ethidium fluorescence (*A*) and Mac-1 immunostaining (*B*) are minimal in the saline-treated mice. By 2 days after MPTP injections, SNpc ethidium fluorescence is increased in WT mice (*C*) and is absent in gp91^{phox}-deficient mice (*E*) and minocycline-treated WT mice (*G*). Microglial activation is prevented by minocycline (*H*) but is normal in gp91^{phox}-deficient mice (*E*). MPTP stimulates NADPH-oxidase activation, as evidenced by p67^{phox} translocation from the cytosol to the plasma membrane in WT mice (wt), but not in gp91^{phox}-deficient mice (ko) (*I* and *J*); the membrane protein calnexin is used to normalize the data. Data are means ± SEM for four to six samples per group. *, $P < 0.05$, higher than controls; #, $P < 0.05$, less than MPTP-injected WT mice, but not different from both saline-injected groups.

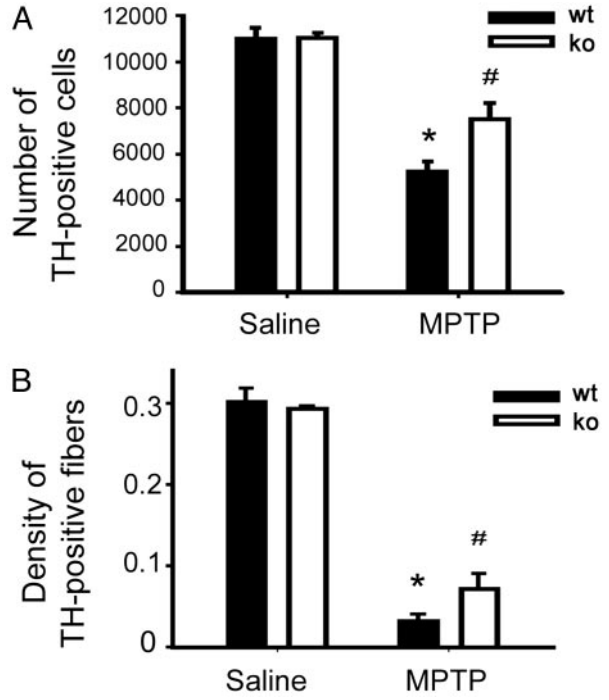

Fig. 5. Stereological counts of TH-positive neurons in the SNpc (*A*) and optical density of striatal DA fibers (*B*) are higher in gp91^{phox}-deficient mice (ko) compared with their WT littermates (wt) 7 days after MPTP injections (n = 4–8 samples per group). *, $P < 0.05$, less than saline-injected mice; #, $P < 0.05$, higher than MPTP-injected WT mice.

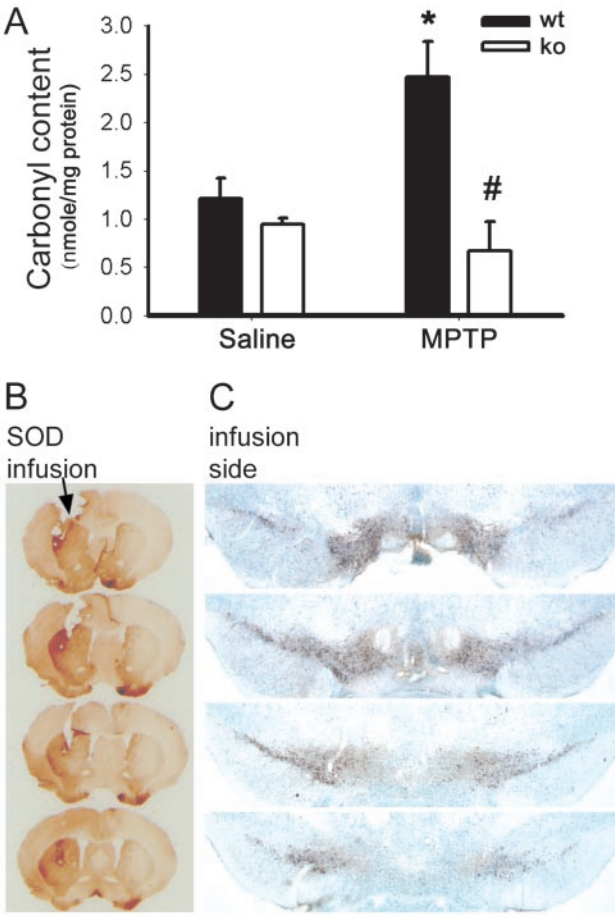

Fig. 6. (*A*) Ventral midbrain carbonyl content, used as a marker of protein oxidative damage, is increased at 2 days after MPTP injections in WT mice (wt), but not in gp91^{phox}-deficient mice (ko). Infusion of SOD1 into the left striatum attenuates the striatal (*B*) and the SNpc lesion on the infused side, but not on the contralateral, noninfused side (*C*) after a systemic injection of MPTP. *, $P < 0.05$, higher than controls; #, $P < 0.05$, less than MPTP-injected WT mice, but not different from the two saline-injected groups.

were reduced in the two groups of animals (Fig. 5*A*). However, the loss was smaller in gp91^{phox}-deficient mice compared with their WT counterparts (Fig. 5*A*). In the striatum of saline-injected mice, the density of TH-positive nerve fibers was similar between gp91^{phox}-deficient mice and their WT littermates (Fig. 5*B*). Like for the number of SNpc TH-positive neurons, in MPTP-injected mice the density of striatal TH-positive nerve fibers was less reduced in the gp91^{phox}-deficient mice than in their WT counterparts (Fig. 5*A*). Because MPTP neurotoxic potency on the nigrostriatal pathway correlates linearly with 1-methyl-4-phenylpyridinium levels in the striatum (14), the content of this active metabolite of MPTP between the two genotypes was evaluated. There were no differences in striatal levels of 1-methyl-4-phenylpyridinium between the gp91^{phox}-deficient mice (17.8 ± 1.4 μg/g striatum; $n = 5$) and WT littermates (17.7 ± 2.0 μg/g striatum; $n = 5$; $P > 0.05$). These results show that NADPH-oxidase participates in the MPTP neurotoxic process affecting DA cell bodies in the SNpc and nerve fibers in the striatum by a mechanism unrelated to an alteration in MPTP toxicokinetics.

NADPH-Oxidase Damages Ventral Midbrain Proteins. To assess the extent of NADPH-oxidase-related oxidative damage, protein carbonyl levels were determined in ventral midbrain of gp91^{phox}-deficient and WT mice after saline or MPTP administration. In saline-injected mice, the levels of ventral midbrain protein carbonyls were similar between the two groups of animals (Fig. 6*A*). In MPTP-injected WT mice, levels of ventral midbrain protein carbonyls were increased (Fig. 6*A*), but in gp91^{phox}-deficient mice they were not different from controls (Fig. 6*A*).

MPTP-Induced Neurotoxicity Is Attenuated by Scavenging Extracellular Superoxide. To test the noxious role of extracellular ROS, the membrane-impermeant enzyme SOD1 was infused into the left striatum. In the MPTP-injected mice, there was a protection of striatal TH-positive fibers on the infused side compared with the noninfused side (Fig. 6*B*). There was also a preservation of SNpc TH-positive cell bodies ipsilateral to the infused side compared with the contralateral noninfused side (Fig. 6*C*). These findings demonstrate the importance of the oxidative stress that emanates from the extracellular space on the demise of neighboring DA neurons.

Discussion

This study shows that the microglial activation in MPTP and PD SNpc specimens is associated with an induction of NADPH-oxidase. This up-regulation correlates topographically and temporally with the DA neurodegenerative changes seen in MPTP mouse and human PD brains. It also parallels the production of ROS seen in the SNpc by 2 days after MPTP injections. The use of minocycline and mutant mice deficient in gp91^{phox} demonstrates collectively that ROS production originates from activated microglia and, within these cells, from NADPH-oxidase.

In the MPTP model, ROS can emanate from both cytosol and mitochondria of DA neurons (15–18). Rise of markers reflecting oxidative damage in the nigrostriatal DA pathway culminates during the first 24 h after MPTP injections (19, 20). In contrast, SNpc NADPH-oxidase-mediated ROS attack becomes signifi-

cant by 2 days after MPTP injections. Therefore, nigrostriatal DA neurons may be subjected first to an intracellular oxidative insult, and then to an extracellular oxidative insult mediated by activated microglia.

Mutant mice deficient in gp91^{phox} exhibited less ventral midbrain protein carbonyl contents and more SNpc DA neurons than their WT littermates after MPTP injections. These results prove that NADPH-oxidase is instrumental in the MPTP neurotoxic process. Activated microglia can also exert deleterious effects unrelated to ROS. Relevant to this notion, mutant mice deficient in gp91^{phox}, despite being defective in NADPH-oxidase, showed no evidence of impaired activation of microglial cells in response to MPTP. Lack of gp91^{phox} expression was also not associated with alteration in the formation of 1-methyl-4-phenylpyridinium, which is the most significant modulator of MPTP potency (14). Therefore, the resistance of gp91^{phox}-deficient mice to MPTP results from the defect of NADPH-oxidase and the consequent reduction of O_2^- formation, and not from either an impaired microglial effector function or an altered MPTP metabolism.

Activated NADPH-oxidase produces O_2^- inward into intracellular vesicles and outward into the extracellular space (8). Neurons located in the vicinity of activated microglial cells may thus have their plasma membrane proteins and lipids exposed to NADPH-oxidase-derived O_2^- and other secondary oxidants, such as hydrogen peroxide. Infusion of SOD1 in the striatum attenuates MPTP-induced loss of striatal DA fibers and SNpc DA neurons; the latter effect may result from a reduction of MPTP-mediated retrograde degeneration (21). This finding indicates that extracellular hydrogen peroxide may not play a great neurotoxic role in the MPTP model, because its formation should have been greatly increased by the combination of infused SOD1 and increased steady-state levels of O_2^- (22) derived from activated NADPH-oxidase. Instead, an increase in the steady-state levels of extracellular O_2^- appears to be pivotal to the killing of SNpc DA neurons.

Among the main isoforms that catalyze NO synthesis, inducible NO synthase is the most closely linked to inflammation. In keeping with this, inducible NO synthase is up-regulated in activated microglial cells both in PD and in the MPTP model (6, 23, 24). In mutant mice deficient in inducible NO synthase, MPTP causes less death of SNpc DA neurons and smaller increases in ventral midbrain nitrotyrosine levels compared with their WT counterparts (6, 24). These findings suggest that a critical part of activated microglial cytotoxicity in the MPTP model and perhaps in PD is also fulfilled by inducible NO synthase-derived NO. Given this, extracellular O_2^- toxicity in the MPTP model could derive from peroxynitrite that is formed by the diffusion-limited reaction of O_2^- with NO (25). Consistent with peroxynitrite involvement in MPTP and PD neurodegenerative processes are the demonstrations that ventral midbrain nitrotyrosine levels are increased after MPTP injections (26, 27), with overexpression of SOD1 preventing the nitration of several important proteins, such as TH (19). α-Synuclein, a presynaptic protein with critical relevance to PD etiopathogenesis, is also nitrated both in the MPTP model and in PD (28, 29).

Activated microglial cells, by generating an extracellular oxidative stress, would likely injure all cells and not solely DA neurons. One way to reconcile the anticipated nonselectivity of the injury with the selectivity of the lesions is to consider that SNpc DA neurons may be particularly vulnerable to extracellular ROS attack compared with the other cells. It is also possible that in the MPTP model and in PD, the magnitude of microglial activation and resulting oxidative stress is mild and only inflicts sublethal lesions. This would succeed in killing only neurons already compromised, as DA neurons probably are in PD and after MPTP injections.

We thank Eric Swanberg and Charles Rohrbach for their expert assistance in quantification of carbonyl contents, Shi-Xuan Wang for assistance with *in situ* hybridization, and the New York Brain Bank at Columbia University for providing the human postmortem samples. This study was supported by National Institutes of Health/National Institute of Neurological Disorders and Stroke Grants NS37345, NS38586, NS42269, NS38370, and NS11766-27AI; National Institutes of Health/National Institute on Aging Grant AG13966; U.S. Department of Defense Grants DAMD 17-99-1-9471 and DAMD 17-03-1; the Lowenstein Foundation; the Lillian Goldman Charitable Trust; and the Parkinson's Disease Foundation. P.T. is the recipient of German Research Foundation Grant TE 343/1-1.

1. Fahn, S. & Przedborski, S. (2000) in *Merritt's Neurology*, ed. Rowland, L. P. (Lippincott, New York), pp. 679–693.
2. Przedborski, S., Kostic, V., Giladi, N. & Eidelberg, D. (2003) in *Dopamine Receptors and Transporters*, eds. Sidhu, A., Laruelle, M. & Vernier, P. (Dekker, New York), pp. 363–402.
3. Chen, H., Zhang, S. M., Hernan, M. A., Schwarzschild, M. A., Willett, W. C. & Colditz, G. A. (2002) *Movement Disorders* **17** (Suppl. 5), S143.
4. Gao, H. M., Jiang, J., Wilson, B., Zhang, W., Hong, J. S. & Liu, B. (2002) *J. Neurochem.* **81,** 1285–1297.
5. Wu, D. C., Jackson-Lewis, V., Vila, M., Tieu, K., Teismann, P., Vadseth, C., Choi, D. K., Ischiropoulos, H. & Przedborski, S. (2002) *J. Neurosci.* **22,** 1763–1771.
6. Liberatore, G., Jackson-Lewis, V., Vukosavic, S., Mandir, A. S., Vila, M., McAuliffe, W. J., Dawson, V. L., Dawson, T. M. & Przedborski, S. (1999) *Nat. Med.* **5,** 1403–1409.
7. Przedborski, S., Jackson-Lewis, V., Vila, M., Wu, D. C., Teismann, P., Tieu, K., Choi, D.-K. & Cohen, O. (2003) in *Parkinson's Disease*, eds. Gordin, A., Kaakkola, S. & Teräväinen, H. (Lippincott, Philadelphia), pp. 83–94.
8. Babior, B. M. (1999) *Blood* **93,** 1464–1476.
9. Przedborski, S., Jackson-Lewis, V., Naini, A., Jakowec, M., Petzinger, G., Miller, R. & Akram, M. (2001) *J. Neurochem.* **76,** 1265–1274.
10. Bindokas, V. P., Jordán, J., Lee, C. C. & Miller, R. J. (1996) *J. Neurosci.* **16,** 1324–1336.
11. Levine, R. L., Garland, D., Oliver, C. N., Amici, A., Climent, I., Lenz, A.-G., Ahn, B.-W., Shaltiel, S. & Stadtman, E. R. (1990) *Methods Enzymol.* **186,** 464–478.
12. Jackson-Lewis, V., Jakowec, M., Burke, R. E. & Przedborski, S. (1995) *Neurodegeneration* **4,** 257–269.
13. Tammariello, S. P., Quinn, M. T. & Estus, S. (2000) *J. Neurosci.* **20,** RC53.
14. Giovanni, A., Sieber, B. A., Heikkila, R. E. & Sonsalla, P. K. (1991) *J. Pharmacol. Exp. Ther.* **257,** 691–697.
15. Przedborski, S., Kostic, V., Jackson-Lewis, V., Naini, A. B., Simonetti, S., Fahn, S., Carlson, E., Epstein, C. J. & Cadet, J. L. (1992) *J. Neurosci.* **12,** 1658–1667.
16. Lotharius, J. & O'Malley, K. L. (2000) *J. Biol. Chem.* **275,** 38581–38588.
17. Hasegawa, E., Takeshige, K., Oishi, T., Murai, Y. & Minakami, S. (1990) *Biochem. Biophys. Res. Commun.* **170,** 1049–1055.
18. Klivenyi, P., St Clair, D., Wermer, M., Yen, H. C., Oberley, T., Yang, L. & Beal, M. F. (1998) *Neurobiol. Dis.* **5,** 253–258.
19. Ara, J., Przedborski, S., Naini, A. B., Jackson-Lewis, V., Trifiletti, R. R., Horwitz, J. & Ischiropoulos, H. (1998) *Proc. Natl. Acad. Sci. USA* **95,** 7659–7663.
20. Mandir, A. S., Przedborski, S., Jackson-Lewis, V., Wang, Z. Q., Simbulan-Rosenthal, M., Smulson, M. E., Hoffman, B. E., Guastella, D. B., Dawson, V. L. & Dawson, T. M. (1999) *Proc. Natl. Acad. Sci. USA* **96,** 5774–5779.
21. Herkenham, M., Little, M. D., Bankiewicz, K., Yang, S. C., Markey, S. P. & Johannessen, J. N. (1991) *Neuroscience* **40,** 133–158.
22. Fridovich, I. (1986) in *Advances in Enzymology*, ed. Meister, A. (Wiley, New York), Vol. 58, pp. 61–97.
23. Hunot, S., Boissière, F., Faucheux, B., Brugg, B., Mouatt-Prigent, A., Agid, Y. & Hirsch, E. C. (1996) *Neuroscience* **72,** 355–363.
24. Dehmer, T., Lindenau, J., Haid, S., Dichgans, J. & Schulz, J. B. (2000) *J. Neurochem.* **74,** 2213–2216.
25. Ischiropoulos, H. & al Mehdi, A. B. (1995) *FEBS Lett.* **364,** 279–282.
26. Schulz, J. B., Matthews, R. T., Muqit, M. M. K., Browne, S. E. & Beal, M. F. (1995) *J. Neurochem.* **64,** 936–939.
27. Pennathur, S., Jackson-Lewis, V., Przedborski, S. & Heinecke, J. W. (1999) *J. Biol. Chem.* **274,** 34621–34628.
28. Przedborski, S., Chen, Q., Vila, M., Giasson, B. I., Djaldatti, R., Vukosavic, S., Souza, J. M., Jackson-Lewis, V., Lee, V. M. & Ischiropoulos, H. (2001) *J. Neurochem.* **76,** 637–640.
29. Giasson, B. I., Duda, J. E., Murray, I. V., Chen, Q., Souza, J. M., Hurtig, H. I., Ischiropoulos, H., Trojanowski, J. Q. & Lee, V. M. (2000) *Science* **290,** 985–989.